LA-10506-MS



Los Alamos National Laboratory is operated by the University of California for the United States Department of Energy under contract W-7405-ENG-36



# Analysis of Tritium Production in a Sphere of LiD Irradiated by 14-MeV Neutrons

Los Alamos Los Alamos National Laboratory
Los Alamos, New Mexico 87545

LA-10506-MS

UC-34C
Issued: August 1985

# Reanalysis of Tritium Production in a Sphere of $^{6}LiD$ Irradiated by 14-MeV Neutrons

L. R. Fawcett, Jr.*



*Collaborator at Los Alamos. Director of Physics and Pre-Engineering Programs, Longwood College, Farmville, VA 23901.

Los Alamos National Laboratory
Los Alamos, New Mexico 87545

CONTENTS

# REANALYSIS OF TRITIUM PRODUCTION IN A SPHERE OF $^{6}$LiD IRRADIATED BY 14-MeV NEUTRONS

by

L. R. Fawcett, Jr.

ABSTRACT

Tritium production and activation of radiochemical detector foils in a sphere of $^{6}$LiD irradiated by a central source of 14-MeV neutrons has been reanalyzed. The $^{6}$LiD sphere consisted of 10 solid hemispherical nested shells with ampules of $^{6}$LiH, $^{7}$LiH, and activation foils located 2.2, 5, 7.7, 12.6, 20, and 30 cm from the center. The Los Alamos Monte Carlo Neutron Photon Transport Code (MCNP) was used to calculate neutron transport through the $^{6}$LiD, tritium production in the ampules, and foil activation. The MCNP input model was three-dimensional and employed ENDF/B-V cross sections for transport, tritium production, and (where available) foil activation. The reanalyzed experimentally observed-to-calculated values of tritium production were 1.053±2.1% in $^{6}$LiH and 0.999±2.1% in $^{7}$LiH. The recalculated foil activation observed-to-calculated ratios were not generally improved over those reported in the original analysis.

---

## I. INTRODUCTION

The objectives of this experiment were (1) to investigate the transport of 14-MeV neutrons through $^{6}$LiD and (2) to determine the production of tritium by these (and all other newborn) neutrons in both $^{6}$Li and $^{7}$Li. The experiment, although similar to the Wyman experiment,[1] differs in that Wyman measured tritium production in $^{7}$Li from neutrons passing through a (natural lithium) LiD sphere.

To accomplish the stated objectives, a 60-cm-diam $^{6}$LiD sphere consisting of a series of nested solid hemispherical shells was assembled with a 14-MeV

neutron source at the center. Integral determination of the neutron energy and flux as a function of distance from the center of the sphere was made by radiochemical detector foils placed on and between the shells at several distances from the source. Tritium production measurements were made with quartz ampules (some filled with $^{6}$LiH and others with $^{7}$LiH) placed between the shells at various distances from the central neutron source. Comparison of reaction rates determined by experiment and calculation tests the ability to calculate the integral over energy of the product of evaluated cross sections and calculated fluxes.

The original analysis of the experiment was reported in 1978.[2] Although in many cases the calculated values for both tritium production and radiochemical activation matched well with the experimental data, in other cases they did not. Since 1978 the capabilities of the transport code have been expanded, and many ENDF/B-V cross sections have been formatted for use in that code. In addition, factors such as room return were not considered in the original analysis, and those factors needed to be investigated. Thus this reanalysis is presented.

## II. EXPERIMENTAL ARRANGEMENT

The report, LA-7310,[2] describes in depth the details of the experiment, and the reader is urged to refer to that document. Only a brief review of salient experimental details is presented here. The $^{6}$LiD consisted of 10 solid hemispherical shells of average density 0.7425 g/cm$^{3}$ and isotopic composition 95.6 (at.%) $^{6}$Li and 4.4 (at.%) $^{7}$Li. These shells were machined so they could be fitted together to form a solid sphere, except for a small spherical cavity at the center to house the tritium target and three small-diameter target access channels. The shell radii were such that radiochemical detector foils could be placed at 2.22, 5, 7.62, 12.6, 20, and 30 cm from the center of the sphere. Quartz ampules filled with $^{6}$LiH ($^{6}$Li 95.5 at.%), $^{7}$LiH ($^{7}$Li 99.9 at.%), and air (for background measurements) were placed in alcoves machined to accommodate them at each of the above radii, except for the 2.22-cm position.

Neutrons (14-MeV) were obtained from the $^{3}$H(d,n)$^{4}$He reaction. A tritium target was placed in the central cavity and 300-keV deuterons from a

Cockcroft-Walton accelerator impinged on the target. The C-W target assembly with some of the nested shells in place around it is shown in Fig. 1.

Figures 2 and 3 show the orientation of the ampules with respect to the deuteron beam. The physical characteristics of the ampules are described in LA-7310. Figure 2 shows the orientation of the foils with respect to the deuteron beam. The foil nuclides were $^{45}Sc$, $^{89}Y$, $^{90}Zr$, $^{169}Tm$, $^{191}Ir$, $^{193}Ir$, $^{197}Au$, $^{235}U$, and $^{238}U$. Details on foil size, thickness, mass, and packaging have been described by G. W. Knobeloch.*

The combination of compound-nucleus recoil and target thickness produced small but possibly significant departures from isotropy in neutron source energy and flux. Before the shells were put into place around the target, the neutron flux was mapped over $4\pi$ sr. For the original analysis the mapped flux and energy anisotropy information was modeled into a neutron source for calculational purposes. The same source routine was used in this reanalysis. The total number of source neutrons was $(9.42\pm0.28)\times10^{15}$.

## III. ANALYSIS

The Los Alamos Monte Carlo Neutron Photon Transport Code (MCNP)[3] was used to calculate neutron transport in the $^{6}LiD$ as well as tritium production in the ampules and foil activation through

$$\int \phi_i(E)\sigma_j(E)dE \ ,$$

where:

$\phi_i$ is the neutron fluence in (neutrons.cm$^{-2}$.MeV$^{-1}$) at ampule or foil position i, and

$\sigma_j$ is the reaction cross section for reaction j.

The geometry of the $^{6}Li$ shells was modeled according to the specifications contained in LA-7310, Part I, Table I. Three small (19, 11.5, and 19 mm diam) channels were cut into the $^{6}Li$ shells to accommodate the $\alpha$ monitor, $^{2}H^{+}$ beam, and cooling tubes (see Fig. 1). These tubes, their channels and

*Information provided by G. W. Knobeloch, Los Alamos Scientific Laboratory office memorandum to D. W. Barr (April 13, 1976).

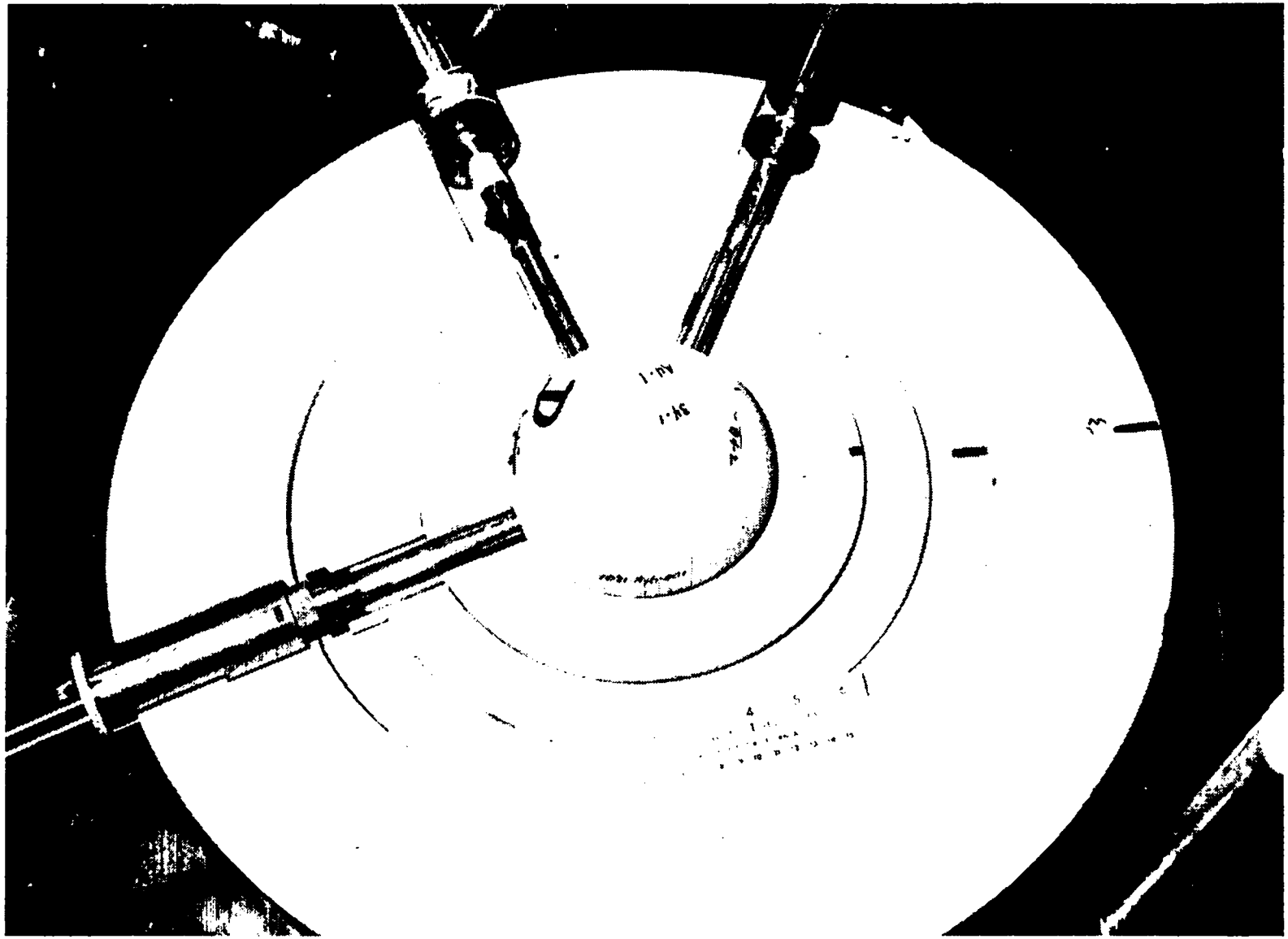

Fig. 1. Partially completed $^{6}LiD$ shell assembly. Clockwise from lower left, the tubes are for target cooling, $^{2}H^{+}$ beam, and $\alpha$ monitor.

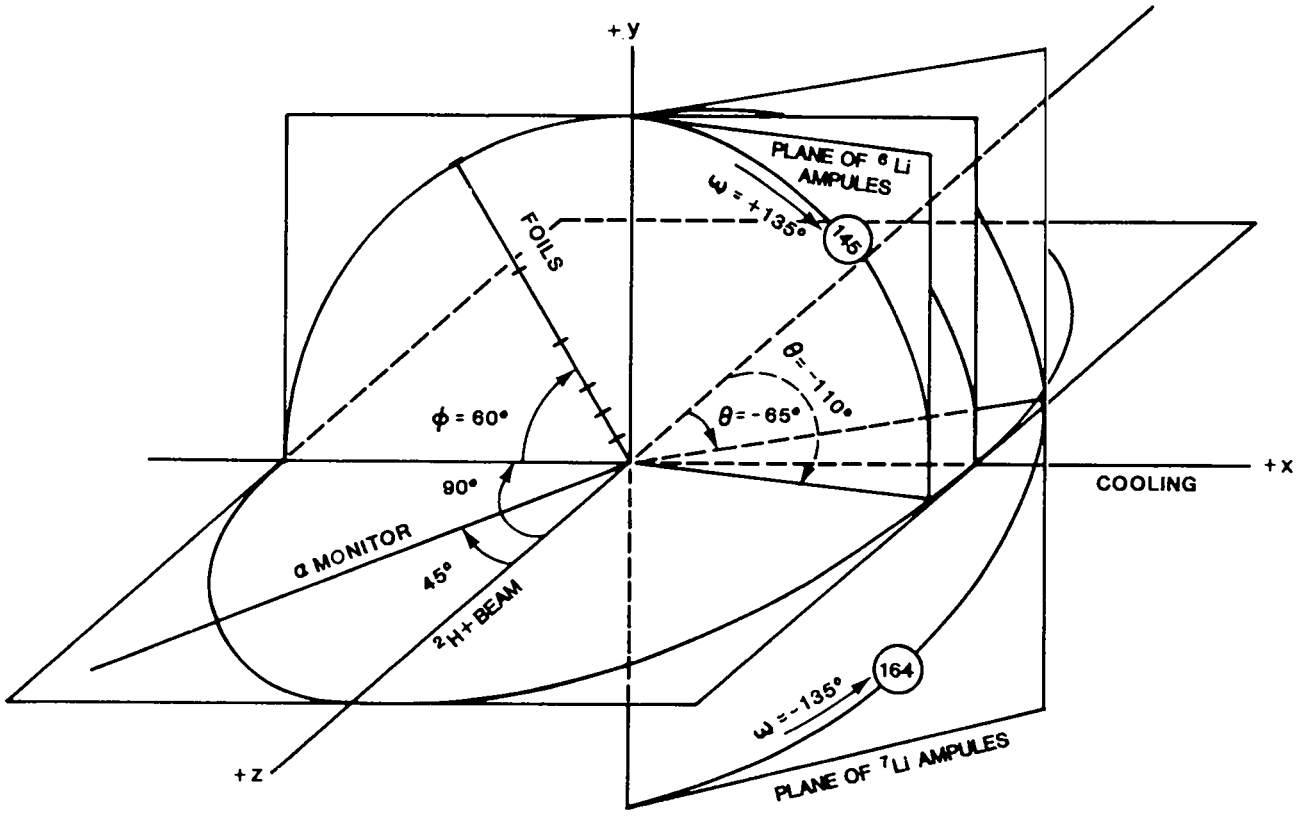


Fig. 2. Orientation of ampule and foil planes. Ampules 145 and 164 are to illustrate how $\omega$ is measured from the x-z plane with $\omega$=0 on the -x side of the y-z plane.

the tritium target wafer were not included in the MCNP model. The justification for their exclusion is based on the fact that this tubing apparatus containing the target wafer was in place when the $4\pi$ sr flux map was measured. Therefore, any disturbance in the 14-MeV flux from neutron penetration of the tubes or target backing is already included in the source routine.

E. Goldberg[4] has independently investigated for this experiment the combined effect of the three channels on tritium production in the ampules and foil activation. Goldberg calculated "channel corrections" for both ampules and foils. Generally these corrections for tritium production were less than 1% except for $^{6}$LiH at the 12.65-cm position, where the correction factor would increase the calculated value by 3%. For foil activation the channel corrections were all 1% or less.

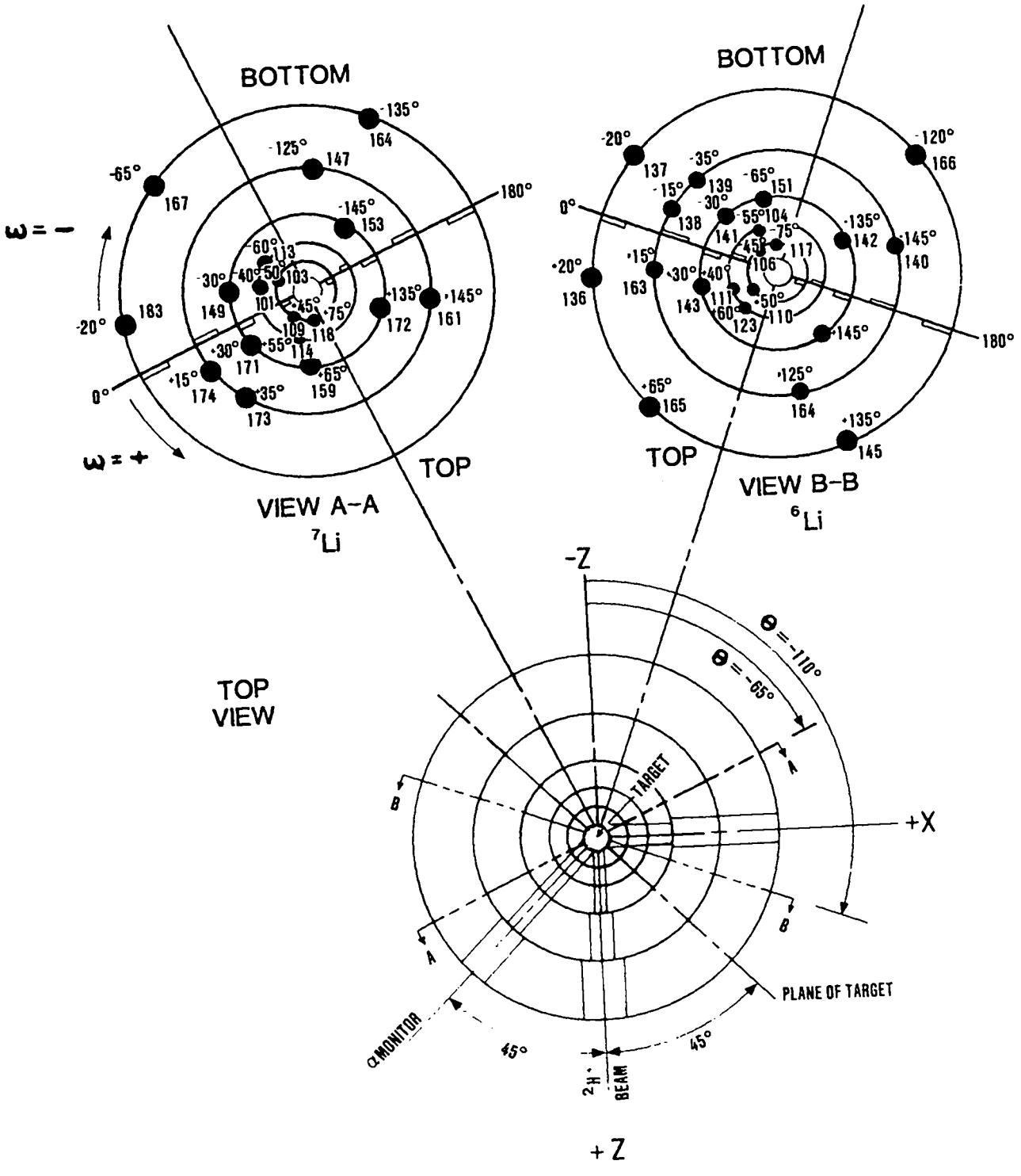


Fig. 3. Orientation of ampules with respect to the $^{2}H^{+}$ beam. In views A-A and B-B, TOP and BOTTOM refer to the actual experimental arrangement.

## A. Tritium Production

All tritium production calculations were three-dimensional, with each ampule modeled for the MCNP input file in the precise experimental location listed later in Table III (Results section). A typical input file is attached as Appendix A. Although the spherical ampules had stems on them, they were treated as spheres without stems to simplify the geometric model. The ampule radii used in the calculations (5 mm at the 5- and 7.7-cm positions and 9 mm at all other positions) matched the outside rather than the inside diameters to make an approximate allowance for stem volume. The LiH mass modeled into each ampule was taken from LA-7310, Part I, Table VI. The quartz shell of approximately 1-mm thickness was not modeled.

Two sets of cross sections were used for both transport and tritium generation. The first set* was the same as those in the original analysis. The purpose of using the same cross sections as used by Jon Wallace[2] was to investigate how well the current calculated values of tritium production would match those of LA-7310. Indeed Table III (Results section), which contains the tritium production, indicates a good match ampule-for-ampule between the results extracted from LA-7310 and the present work for $^{7}Li$. The match is poor for $^{6}Li$ ampules at the 7.7- and 30-cm radial positions in that the calculated values between this and the earlier work differ by 14% to 40%.

The large mismatch at these two radial positions was expected. In the original analysis,[2] to improve statistics the ampule radii were increased from 5 to 6 mm and 9 to 15.3 mm in the 7.7-cm and 30-cm positions respectively without changing the $^{6}LiH$ density. Thus, the amount of hydrogen in these ampules was increased in the transport calculations. This extra hydrogen caused an artificial overmoderating effect in these ampules that significantly increased the calculated tritium production by folding an increased population of slower neutrons with correspondingly higher $^{6}Li(n,t)\alpha$ cross sections. A similar effect is suppressed in $^{7}LiH$-filled ampules because the $^{7}Li$ tritium production cross section has a 2.8-MeV threshold. A sensitivity study in the current work indicates the degree of importance for $^{6}LiH$-filled ampules to be modeled with the correct mass of $^{6}LiH$. An MCNP run

*ENDF/B-III cross-section sets were employed for both transport and tritium production except for $^{2}H$, for which the 1967 UK/Los Alamos evaluation was used for transport.

showed that increasing the radius of the outermost ampules from 0.9 cm to 2 cm without adjusting the $^{6}$LiH density to keep the mass constant resulted in a greater than 30% increase in the calculated value for tritium production per $^{6}$Li atom.

The second set of cross sections used for both transport and tritium generation was from the ENDF/B-V evaluation.* It is upon these cross sections that this reanalysis is based.

The isotopic abundance in the $^{7}$LiH ampules was 99.9% $^{7}$Li and 0.1% $^{6}$Li. In the calculations the $^{7}$Li ampules were treated as if they contained 100% $^{7}$Li. The isotopic abundance in the $^{6}$LiH ampules was 95.5% $^{6}$Li and 4.5% $^{7}$Li. In this case the 4.5% $^{7}$Li and 95.5% $^{6}$Li tritium production contributions were calculated and added so that the calculational model matched the experiment precisely.

## B. Radiochemical Detector Foils

The radiochemical activation calculations were three-dimensional (using point detectors) for neutron energies above 0.1 MeV and one-dimensional (using surface tallies) for energies below 0.1 MeV. Thus, the calculated values of foil activation consist of the sum of two calculations. Of course, one would prefer to use the three-dimensional model over all neutron energies. However, the point detectors require prohibitive amounts of computer time per neutron history when neutrons are followed into the lower energy ranges.

The two-part calculation is thought to be justified on the premise that the downscattered neutron fluence approaches isotropy. In the original analysis, point detectors were used for energies above 7.4 MeV and surface tallies below 7.4 MeV.[2]

Point detectors, which were modeled in the input file at the experimental coordinates of the foils, tally the neutron fluence at the detector location. A surface tally produces an integrated fluence over an entire

*ENDF/B-V cross sections were used for transport and tritium production, except for $^{2}$H and $^{7}$Li, for which the 1982 Los Alamos Group T-2 evaluations were employed. The Group T-2 evaluation for $^{7}$Li is the same as ENDF/B-V Revision 2. The $^{2}$H evaluation is the same as ENDF/B-V except the library used here has been updated with correlated energy angular distribution for the (n,2n) reaction.

surface. To obtain acceptable statistics, the point detector runs required 100 000 histories; the surface tally runs required at least 200 000 histories and in some cases as many as 600 000.

In general, two sets of cross sections were used for both transport and radiochemical foil activation. The first set was the same as those used in the original work[2] except for $^{89}Y(n,\gamma)$ activation in which a file was prepared for MCNP that was similar to that used in LA-3710.* Again, the purpose of using the same cross sections as were used in the previous analysis was to investigate how well the current calculated values would match those obtained by Jon Wallace[2]. Appendix B is a comparison of the experimentally observed-to-calculated ratios between this work (based on cross sections from the previous analysis) and the results in LA-7310.

The second set of cross sections used for transport throughout this reanalysis was from the ENDF/B-V evaluation. ENDF/B-V cross sections were also used for activation in those cases where they were available. In cases where ENDF/B-V dosimetry cross sections were not available or other dosimetry cross sections were used in addition to those of ENDF/B-V, those cross sections are identified in Tables V & VI in the Results section.

## C. Perturbations

The effects of several physical phenomena were automatically included in the experimental results. These phenomena were investigated in the theoretical analysis to determine whether their influences on the system were large enough to be included as corrections to the calculated values.

### 1. Self- and Cross-Activation

In the foil positions close to the neutron source, some foils were packaged on top of one another to conserve space. Thus not only would there be self-activation of a foil from neutrons born within it, but also cross-activation from neutrons born in the superimposed foil penetrating the first

*File provided by R. C. Little and R. E. Seamon, Los Alamos National Laboratory, "Cross Sections for $^{89}Y(n,\gamma)$," memorandum to L. R. Fawcett, Jr. (July 21, 1981).

foil. The magnitude of self- and cross-activation was calculated for radiative capture (using MCNP) in the innermost position, where the effect was expected to be most pronounced because the 14-MeV flux component was highest and thereby permitted neutron production from high-threshold reactions. In the 2.22-cm position $^{197}Au$ and $^{238}U$ foils were packaged on top of each other. The following contributions from neutrons born in these foils were considered:

a. (n,γ) activation in $^{238}U$ and $^{197}Au$ from fission neutrons born in $^{238}U$,

b. (n,γ) activation in $^{238}U$ and $^{197}Au$ from (n,2n) neutrons born in $^{238}U$.

c. (n,γ) activation in $^{238}U$ and $^{197}Au$ from (n,3n) neutrons born in $^{238}U$, and

d. (n,γ) activation in $^{238}U$ and $^{197}Au$ from (n,2n) neutrons born in $^{197}Au$.

When contributions a. through d. were added and compared to the total activation from all other neutrons, it was found that the self- and cross-activation effects were small: $^{238}U(n,\gamma)$, 1.9% and $^{197}Au(n,\gamma)$, 1.1%. Nevertheless, these corrections are included in Tables V and VI in the Results section. Contributions a. through d. were also calculated for (n,f) in $^{238}U$ at the 2.22-cm position. The effect was very small (0.1%). Self- and cross (n,2n)-activations were not calculated because the vast majority of newborn neutrons have energies below the threshold for the (n,2n) reaction in $^{197}Au$ and $^{238}U$.

## 2. Room Return

The experiment was performed in a large steel and concrete room. The room was measured with respect to the location of the $^{6}LiD$ sphere and modeled for MCNP. Structures and equipment around the sphere were not included in the model. The calculated contribution to the activation of the outermost foils from neutrons that escaped the sphere and later returned was less than 1% for the several materials and reactions considered. The room return contributions are summarized in Table I. Because these contributions are less than 1%, they are not included in the radiochemical activation results presented in Tables V and VI (Results section).

## TABLE I

### ROOM RETURN

### FRACTIONAL CONTRIBUTION TO ACTIVATION OF THE FOILS AT 30 CM

| Nuclide | Reaction[a] | Fractional Contribution |
|---|---|---|
| $^{235}U$ | (n,f) | .0023 |
| $^{238}U$ | (n,f) | .0004 |
| $^{45}Sc$ | (n,γ) | .0062 |
| $^{89}Y$ | (n,γ) | .0072 |
| $^{169}Tm$ | (n,γ) | .0076 |
| $^{197}Au$ | (n,γ) | .0064 |
| $^{238}U$ | (n,γ) | .0056 |

[a]The high-threshold energy (n,2n) reactions were not considered because returning neutrons are likely to be degraded in energy.

### 3. Off-Center Source

It cannot be determined whether the neutron source was off center; however, observed-to-calculated ratios consistently larger than unity for the (n,2n) activations in the 2.22-cm position (see Table VI, Results section) lead one to consider the possibility of the source being closer to the foils than it was supposed to have been. Monte Carlo calculations were made for selected foils where the neutron source was positioned off center such that it was 2 mm closer to the foils. The "on-center" and "off-center" calculations are compared in Table II and discussed in the section on results.

### 4. Charged Particle Production

It is well known that when 14-MeV neutrons penetrate $^{6}LiD$, abundant high-energy charged particles are produced. Some of these charged particles

## TABLE II

### SOURCE OFF-CENTER COMPARISONS
### (For Source 2 mm Closer to Foils)

### OBSERVED-TO-CALCULATED RADIOCHEMICAL ACTIVATIONS

| Reaction | Neutron Source Position | Foil Distance From Sphere Center (cm) | | | |
|---|---|---|---|---|---|
| | | 2.22 | 5 | 7.62 | 12.6 |
| $^{89}Y(n,2n)$ | CENTERED | 1.255 | 1.003 | 1.000 | 0.953 |
| | 2 mm | 1.039 | 0.915 | 0.968 | 0.886 |
| $^{197}Au(n,2n)$ | CENTERED | 1.140 | 0.986 | 0.892 | 0.958 |
| | 2 mm | 0.944 | 0.895 | 0.876 | 0.901 |
| $^{238}U(n,2n)$ | CENTERED | 1.168 | 1.148 | 1.075 | 1.111 |
| | 2 mm | 0.969 | 1.054 | 1.064 | 1.104 |
| $^{238}U(n,f)$ | CENTERED | 1.253 | 1.068 | 1.037 | 1.075 |
| | 2 mm | 1.040 | 0.984 | 0.985 | 1.052 |
| $^{197}Au(n,\gamma)$ | CENTERED | 1.522 | 1.327 | 1.166 | 1.046 |
| | 2 mm | 1.480 | 1.311 | 1.143 | 1.060 |
| $^{238}U(n,\gamma)$ | CENTERED | 1.477 | 1.265 | 1.135 | 1.005 |
| | 2 mm | 1.394 | 1.242 | 1.114 | 1.020 |

interact with $^{6}LiD$ to produce secondary neutrons. Indeed we have calculated the charged particle production for this $^{6}LiD$ sphere. For each source neutron, 4.5 deuterons, 1.4 alphas, 0.8 tritons, and 0.25 protons are produced. Unfortunately MCNP, as currently constructed, does not transport charged particles. Therefore, the number of new neutrons produced by these charged particles is unknown but could have been significant in the experimental results.

### D. Errors

Values calculated by the MCNP Transport Code are accompanied by a statistical error corresponding to one fractional standard deviation of the mean. No estimates of cross-section uncertainties are included. The precisions of the experimental values were taken from D. W. Barr[5] and LA-7310.

These are the uncertainties assigned to observed and calculated values found in Tables III and V (Results section). In addition, for tritium production the experimenters estimated 6% systematic error in the observed values[2] because of normalizations and the standard deviation in the neutron source strength. Generally the errors quoted on observed-to-calculated ratios are for one fractional standard deviation and consist of the square root of the sum of the squared experimental and calculated fractional errors. When uncertainties were derived by other formulations, the method is explained by footnotes to the tables.

## IV. RESULTS

### A. Tritium Production

Table III contains the tritium production for each ampule and the corresponding observed-to-calculated ratios. The layout of the table is such that one may readily compare the calculated values from LA-7310 with those of the present work. Whereas specific tritium production, f(r), is reported in LA-7310, the absolute tritium production, N, is reported here. Absolute tritium production is defined as the number of tritons produced per Li atom in an ampule for the total number of source neutrons. Specific and absolute tritium production are related by

$$N = \frac{f(r)n}{4\pi r^2} ,$$

where

f(r) is in units of $\frac{\text{tritons produced} \cdot \text{mm}^2}{\text{Li atom} \cdot \text{source neutron}}$

n is the number of source neutrons, and

r is the distance from the neutron source to the center of an ampule in mm.

Table III shows that ENDF/B-V cross sections did not improve observed-to-calculated ratios in $^6$Li over those where LA-7310 cross sections were used in the present work. The improvement in $^6$Li ratios came about by calculating

TABLE III

TRITIUM PRODUCTION - OBSERVED AND CALCULATED[a]

| Li Isotope | Sample No | Location r (mm) | Location ω[b] (deg) | N(Obs)[c] x $10^{13}$ Experiment (Tritons Produced / Li Atom) | N(Calc)[d] x $10^{13}$ LA-7310 (Tritons Produced / Li Atom) | N(Calc)[e] x $10^{13}$ Present Work LA-7310 σ's (Tritons Produced / Li Atom) | N(Calc)[f] x $10^{13}$ Present Work ENDF/B-V σ's (Tritons Produced / Li Atom) | Observed / Calculated LA-7310 | Observed[g] / Calculated Present Work LA-7310 σ's | Observed[g] / Calculated Present Work ENDF/B-V σ's |
|---|---|---|---|---|---|---|---|---|---|---|
| 6 | 136 | 299.5 | 20 | 2.06 ± 6% | 2.53 | 1.94 ± 9.1% | 2.10 ± 8.6% | 0.814 | 1.06 ± 11% | 0.981 ± 10% |
| | 137 | 299.5 | - 20 | 2.29 ± 6% | 2.56 | 1.83 ± 7.5% | 1.91 ± 6.9% | 0.896 | 1.25 ± 10% | 1.20 ± 9% |
| | 145 | 299.5 | 135 | 2.81 ± 6% | 2.35 | 1.76 ± 7.5% | 2.08 ± 10.9% | 1.20 | 1.60 ± 10% | 1.35 ± 12% |
| | 138 | 201.5 | - 15 | 14.3 ± 6% | 15.0 | 14.0 ± 3.9% | 14.3 ± 3.7% | 0.950 | 1.02 ± 7% | 1.00 ± 7% |
| | 139 | 201.5 | - 35 | 15.0 ± 6% | 14.0 | 14.8 ± 4.1% | 13.6 ± 3.8% | 1.07 | 1.01 ± 7% | 1.10 ± 7% |
| | 140 | 201.5 | -145 | 15.0 ± 6% | 14.5 | 14.5 ± 4.3% | 14.6 ± 3.8% | 1.03 | 1.03 ± 7% | 1.03 ± 7% |
| | 141 | 127.5 | - 30 | 37.6 ± 6% | 36.6 | 37.9 ± 3.0% | 35.7 ± 3.3% | 1.03 | 0.992 ± 7% | 1.05 ± 7% |
| | 142 | 127.5 | -135 | 36.4 ± 6% | 33.9 | 35.8 ± 3.1% | 36.0 ± 3.2% | 1.07 | 1.02 ± 7% | 1.01 ± 7% |
| | 143 | 125.5 | 30 | 41.7 ± 6% | 35.9 | 37.9 ± 3.1% | 37.8 ± 3.4% | 1.16 | 1.10 ± 7% | 1.10 ± 7% |
| | 104 | 77.64 | - 55 | 63.9 ± 6% | 74.2 | 65.2 ± 4.6% | 64.0 ± 4.7% | 0.861 | 0.980 ± 8% | 0.992 ± 7% |
| | 111 | 76.66 | 40 | 65.2 ± 6% | 75.4 | 61.6 ± 4.2% | 63.5 ± 4.3% | 0.865 | 1.06 ± 7% | 1.03 ± 7% |
| | 106 | 51.2 | - 45 | 103 ± 6% | 95.5 | 99.0 ± 3.6% | 96.5 ± 3.8% | 1.08 | 1.04 ± 7% | 1.07 ± 7% |
| | 110 | 49.5 | 50 | 101 ± 6% | 101 | 98.9 ± 3.8% | 94.1 ± 3.5% | 1.00 | 1.02 ± 7% | 1.07 ± 7% |
| 7 | 183 | 299.5 | - 20 | 0.949 ± 6% | 1.00 | 1.01 ± 6.7% | 0.911 ± 6.7% | 0.949 | 0.940 ± 9% | 1.04 ± 9% |
| | 186 | 299.5 | 120 | 0.937 ± 6% | 0.911 | 0.908 ± 7.3% | 0.864 ± 7.2% | 1.03 | 1.03 ± 9% | 1.08 ± 9% |
| | 147 | 201.5 | -125 | 3.40 ± 6% | 3.93 | 3.92 ± 4.8% | 3.64 ± 4.8% | 0.863 | 0.867 ± 8% | 0.926 ± 8% |
| | 173 | 199.5 | 35 | 3.87 ± 6% | 3.97 | 3.63 ± 5.2% | 3.27 ± 5.0% | 0.973 | 1.07 ± 8% | 1.18 ± 8% |
| | 149 | 127.5 | - 30 | 11.7 ± 6% | 13.6 | 13.8 ± 3.2% | 12.0 ± 3.3% | 0.858 | 0.846 ± 7% | 0.973 ± 7% |
| | 171 | 125.5 | 30 | 11.9 ± 6% | 13.5 | 13.9 ± 3.3% | 12.4 ± 3.3% | 0.884 | 0.855 ± 7% | 0.960 ± 7% |
| | 172 | 125.5 | 135 | 11.9 ± 6% | 12.8 | 13.6 ± 3.2% | 11.9 ± 3.3% | 0.930 | 0.876 ± 7% | 1.00 ± 7% |
| | 101 | 77.68 | - 40 | 38.5 ± 6% | 42.7 | 45.9 ± 3.3% | 40.4 ± 3.3% | 0.900 | 0.839 ± 7% | 0.953 ± 7% |
| | 114 | 75.66 | 55 | 38.3 ± 6% | 46.5 | 46.1 ± 3.2% | 41.0 ± 3.3% | 0.823 | 0.831 ± 7% | 0.934 ± 7% |
| | 103 | 49.5 | - 50 | 91.7 ± 6% | 106 | 113 ± 2.0% | 99.2 ± 2.1% | 0.861 | 0.812 ± 6% | 0.924 ± 6% |
| | 109 | 51.5 | 45 | 91.0 ± 6% | 101 | 103 ± 2.1% | 89.6 ± 2.2% | 0.904 | 0.883 ± 6% | 1.02 ± 6% |

[a] The quoted uncertainities on both observed and calculated values are for one fractional standard deviation. In addition, there is an estimated 6% systematic error in the observed values which is not factored into the errors quoted here.

[b] Angles above the parting plane in the experimental configuration are positive; angles below the parting plane are negative.

[c] Observed tritium production extracted from LA-7310, Table VI, p.12, (Tritons produced per Li atom by 9.42 x $10^{15}$ source neutrons.)

[d] Calculated tritium production extracted from LA-7310, Tables VII and IX, pp.22-23. (Tritons produced per Li atom by 9.42 x $10^{15}$ source neutrons.)

[e] Tritium production calculated in this work using ENDF/B-III cross section data for both transport and tritium production except for $^{2}H$ in which the 1967 UK/Los Alamos evaluation was employed in transport. (Tritons produced per Li atom by 9.42 x $10^{15}$ source neutrons.)

[f] Tritium production calculated in this work using ENDF/B-V cross section data for both transport and tritum production. (Tritons produced per Li atom by 9.42 x $10^{15}$ source neutrons.)

[g] The quoted errors were determined from a square root of the sum of the squares combination of the observed and calculated uncertainties.

with ampules at positions 7.7 and 30 cm which contained the correct mass of $^{6}$LiH. For $^{7}$Li, the improvement in ratios is due to the use of ENDF/B-V cross sections.

Where ENDF/B-V cross sections were used for both transport and production, the observed-to-calculated ratios are unity within the limits of the quoted uncertainties for 9 of 13 $^{6}$LiH ampules and 9 of 11 $^{7}$LiH ampules.

Inspection of the column headed N(OBS) in Table III shows that the experimental value of tritium production per $^{6}$Li atom in ampule 145 was 29% greater than that of the average of the other ampules at 299.5 mm. In no other case was there an experimental variation between ampules (at a given radius) anywhere close to this magnitude. There is no known reason why the measured value of tritium generation in ampule 145 should differ from that of the other ampules at the 299.5-mm position. It was not because 145 had the best view of the floor. Ampule 145 was on the top hemishell. We believe that ampule 145 should be excluded from the data base.

The average observed-to-calculated tritium production ratio that assigns equal weight to each ampule is obtained by averaging the observed-to-calculated ratios for a particular Li isotope. When ENDF/B-V cross sections were used for transport and production, the average ratio for $^{6}$Li (excluding ampule 145) is

$$\overline{(\text{Obs./Calc.})}_{\text{t in } ^{6}\text{LiH}} = 1.053 \pm 2.1\%^{*}$$

The average ratio for $^{7}$Li (including all ampules) is

$$\overline{(\text{Obs./Calc.})}_{\text{t in } ^{7}\text{LiH}} = 0.999 \pm 2.1\%^{*}$$

The information presented in Table III is summarized in Table IV by presenting the average tritium production at each radius. In the present work with ENDF/B-V cross sections, the observed-to-calculated ratios for $^{6}$Li range between 1.01 and 1.09. For $^{7}$Li they lie between 0.943 and 1.06. If ampule 145 is omitted, the O/C ratios are unity within the limits of the quoted uncertainties in 6 of 10 cases. From Table IV it is evident that the use of ENDF/B-V cross sections results in improved observed-to-calculated ratios for $^{7}$Li.

*This uncertainty, determined by the formulation in note e of Table IV, does not include the 6% systematic error in the observed values.

TABLE IV

AVERAGE TRITIUM PRODUCTION AT EACH RADIUS -- OBSERVED AND CALCULATED[a]

| Li Isotope | Distance From Source r (mm) | N(Obs)[b,c] x $10^{13}$ Experiment (Tritons Produced / Li Atom) | N(Calc)[c,d] x $10^{13}$ Present Work LA-7310 σ's (Tritons Produced / 1I Atom) | N(Calc)[c,e] x $10^{13}$ Present Work ENDF/B-V σ's (Tritons Produced / 1I Atom) | Observed[f] / Calculated Present Work LA-7310 σ's | Observed[f] / Calculated Present Work ENDF/B-V σ's |
|---|---|---|---|---|---|---|
| 6 | 50 | 102 ± 4.2% | 99.0 ± 2.6% | 95.3 ± 2.6% | 1.03 ± 4.9% | 1.07 ± 4.9% |
| | 77 | 64.5 ± 4.2% | 63.4 ± 3.1% | 64.9 ± 3.2% | 1.02 ± 5.2% | 1.01 ± 5.3% |
| | 127 | 38.6 ± 3.5% | 37.2 ± 1.7% | 37.6 ± 1.9% | 1.04 ± 3.9% | 1.05 ± 4.0% |
| | 201 | 14.8 ± 3.5% | 14.4 ± 2.4% | 14.7 ± 2.2% | 1.03 ± 4.2% | 1.04 ± 4.1% |
| | 300 | 2.39 ± 3.4% | 1.84 ± 4.5% | 2.08 ± 4.7% | 1.30 ± 5.6% | 1.18 ± 5.8% |
| | 300[g] | 2.18 ± 4.3% | 1.89 ± 5.9% | 2.06 ± 5.5% | 1.15 ± 7.3% | 1.09 ± 7.0% |
| 7 | 50 | 91.4 ± 4.2% | 108 ± 1.4% | 94.4 ± 1.6% | 0.846 ± 4.4% | 0.968 ± 4.5% |
| | 77 | 38.4 ± 4.2% | 46.0 ± 2.3% | 40.7 ± 2.3% | 0.835 ± 4.8% | 0.943 ± 4.8% |
| | 127 | 11.8 ± 3.5% | 13.8 ± 1.9% | 12.1 ± 1.9% | 0.855 ± 4.0% | 0.975 ± 4.0% |
| | 201 | 3.64 ± 4.2% | 3.78 ± 3.5% | 3.47 ± 3.5% | 0.963 ± 5.5% | 1.05 ± 5.5% |
| | 300 | 0.943 ± 4.2% | 0.959 ± 4.9% | 0.888 ± 5.0% | 0.983 ± 6.5% | 1.06 ± 6.5% |

[a]The quoted uncertainties on both observed and calculated values are for one fractional standard deviation. In addition, there is a 6% systematic error in the observed values.

[b]Observed tritium production (tritons produced per Li atom by 9.42 x $10^{15}$ source neutrons).

[c]The errors assigned to the observed and calculated averages were determined using:[6]

$$s = \left( \frac{1}{\sum \frac{1}{s_i^2}} \right)^{1/2}$$

[d]Tritium production calculated in this work using ENDF/B-III cross-section data for both transport and tritium production, except for $^{2}H$, where the 1967 UK/Los Alamos evaluation was employed in transport. (Tritons produced per Li atom by 9.42 x $10^{15}$ source neutrons.)

[e]Tritium production calculated in this work using ENDF/B-V cross-section data for both transport and tritium production. (Tritons produced per Li atom by 9.42 x $10^{15}$ source neutrons.)

[f]The quoted errors were determined from a square root of the sum of the squares combination of the observed and calculated uncertainties.

[g]Ampule 145 is omitted from these calculations.

In Fig. 4 the average observed-to-calculated ratios obtained in the present work using ENDF/B-V cross sections are compared with calculation IV from LA-7310, Part II, Tables VI and VIII. For $^{6}Li$ the ratios from the current work, although greater than unity, are more consistently close to one than are those of LA-7310. That is, the present work exhibits less scatter. For $^{7}Li$ the present results, although exhibiting somewhat more scatter than those of LA-7310, are in general much closer to unity.

## B. Radiochemical Detector Foils

Except for the neutron source routine, the MCNP input model was constructed independently of that of the original analysis. It was felt that if

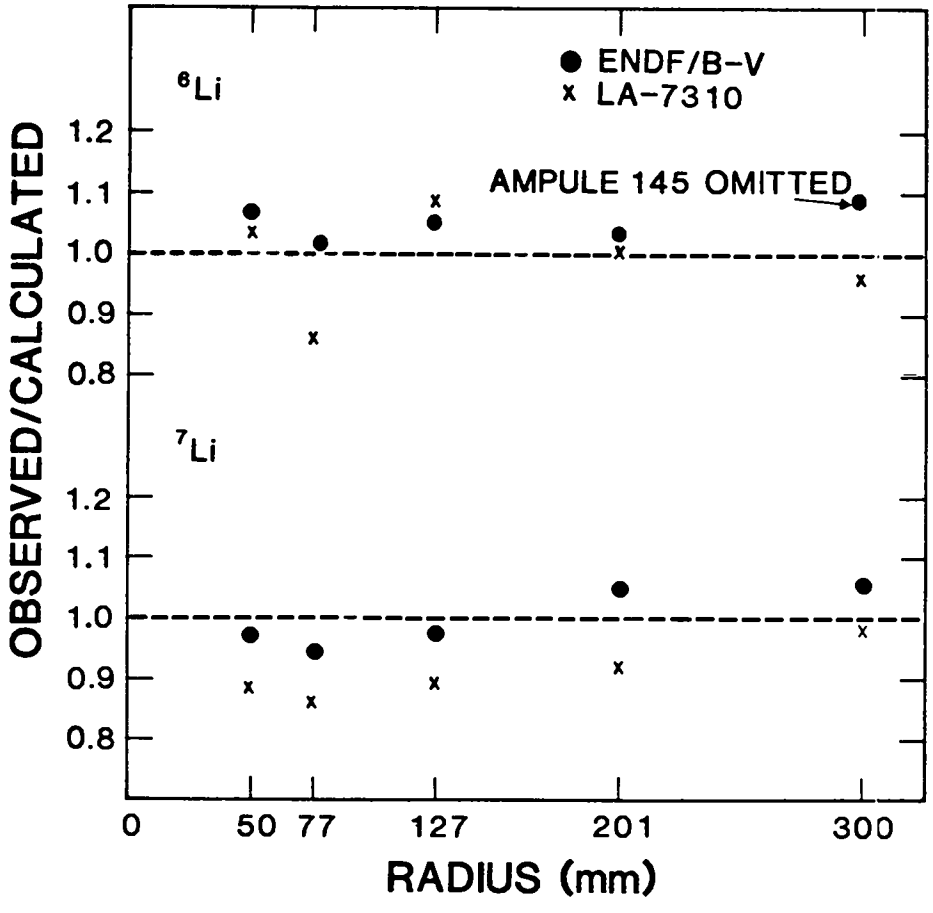


Fig. 4. Average observed-to-calculated tritium production at each radius. The present work is based on ENDF/B-V cross sections for transport and production. The LA-7310 values were taken from calculation IV of Tables VI and VII in Part II of that document.

the previous results could be reproduced, that would lend weight to the validity of the present model. When the same cross sections as those of LA-7310 were used, the calculated radiochemical activation values produced observed-to-calculated ratios similar to those of the previous analysis. A perusal of Appendix B shows that in only 2 of 81 cases do the ratios differ by more than 10%. Usually, the ratios match within 1 or 2%. The overall averaged observed-to-calculated ratios were 1.031 for the original work and 1.011 for the present work using the same cross sections.

At this point it was expected that calculations with the more recent ENDF/B-V cross-section evaluations would result in improved individual observed-to-calculated ratios. Such was not true. The results of the recalculation are presented in Tables V and VI. Table V contains the experimental and calculated values. Table VI is more interesting because the calculated values are compared with experiment through observed-to-calculated ratios. Although the most up-to-date ENDF/B-V cross sections were used for transport throughout (and for foil activation when they were available), the results are in many cases unsatisfactory. The use of ENDF/B-V activation cross sections did not generally improve the results and for Au(n,$\gamma$) made them worse. Approximately 1/3 of the observed-to-calculated ratios still differ from unity by more than 10%.

### 1. (n,2n) Activation

These reactions are the most troublesome in that the results all fail in the same way. The observed-to-calculated ratios are larger than unity in the 2.2-cm position and generally decrease to values substantially less than unity in the 30-cm position. (See n,2n, Fig. 5.) Even calculated values from alternative activation cross sections for $^{197}$Au(n,2n) and $^{238}$U(n,2n) did not mitigate the problem. Nevertheless, part of the difficulty may lie with the (n,2n) cross sections. A cross section with smaller positive slope near the reaction threshold and a larger positive slope near 14 MeV would decrease the calculated values at deep penetration and increase them close to the source, where 14-MeV neutrons predominate.

Possibly the neutron transport cross sections may not be degrading the energy of deep penetration source neutrons quite soon enough. Small

TABLE V

RADIOCHEMICAL ACTIVATION
EXPERIMENTALLY OBSERVED[a] AND CALCULATED[b] VALUES ($\times 10^{13}$)
(ENDF/B-V TRANSPORT CROSS SECTIONS)

| Reaction | Activation[c,d] Cross Section | Notes | Distance from Source (cm) 2.22 | 5.00 | 7.615 | 12.60 | 20.00 | 30.00 |
|---|---|---|---|---|---|---|---|---|
| $^{89}Y(n,2n)$ | | Experiment[e] | 1665 ± 3%[f] | 219.2 ± 3% | 76.75 ± 3% | 18.02 ± 3% | 3.999 ± 3% | 0.6924 ± 3% |
| | 39089.713 | Calculated[g] | 1327 ± 0% | 218.5 ± 2% | 76.22 ± 2% | 18.91 ± 5% | 4.019 ± 2% | 0.7702 ± 3% |
| $^{90}Zr(n,2n)$ | | Experiment | | 145.0 ± 3% | 49.78 ± 3% | 11.44 ± 3% | 2.131 ± 4% | 0.3561 ± 9% |
| | 40090.703 | Calculated | | 150.7 ± 2% | 51.80 ± 2% | 12.35 ± 4% | 2.522 ± 2% | 0.4630 ± 3% |
| $^{169}Tm(n,2n)$ | | Experiment | | 528.6 ± 3% | 197.4 ± 3% | 55.00 ± 3% | 13.62 ± 3% | 2.935 ± 3% |
| | 69169.713 | Calculated | | 538.7 ± 2% | 202.7 ± 3% | 55.95 ± 5% | 14.02 ± 3% | 3.208 ± 2% |
| $^{191}Ir(n,2n)$ | | Experiment | | 534.7 ± 3% | 197.6 ± 3% | 51.15 ± 3% | 12.70 ± 3% | 2.660 ± 7% |
| | 77191.713 | Calculated | | 535.3 ± 1% | 221.3 ± 3% | 55.15 ± 2% | 15.14 ± 7% | 3.253 ± 3% |
| $^{197}Au(n,2n)$ | | Experiment | 3916 ± 3% | 578.3 ± 3% | 214.8 ± 3% | 56.88 ± 3% | 13.87 ± 3% | 2.994 ± 3% |
| | 79197.713 | Calculated | 3453 ± 0% | 591.1 ± 1% | 243.2 ± 3% | 60.23 ± 2% | 16.41 ± 7% | 3.487 ± 3% |
| | 79197.50 | Calculated | 3436 ± 0% | 586.4 ± 1% | 240.7 ± 3% | 59.37 ± 2% | 16.11 ± 7% | 3.405 ± 3% |
| $^{238}U(n,2n)$ | | Experiment | 1540 ± 3% | 295.9 ± 3% | 118.7 ± 3% | 37.13 ± 3% | 10.88 ± 3% | 2.733 ± 5% |
| | 92238.713 | Calculated | 1345 ± 0% | 265.7 ± 2% | 115.1 ± 5% | 35.10 ± 5% | 9.877 ± 3% | 2.956 ± 9% |
| | 92238.50 | Calculated | 1318 ± 0% | 257.7 ± 2% | 110.4 ± 5% | 33.43 ± 4% | 9.376 ± 3% | 2.789 ± 9% |
| $^{193}Ir(n,2n)$ | | Experiment | | 401.1 ± 3% | 166.8 ± 3% | 52.30 ± 3% | 16.20 ± 3% | 2.97 ± 7% |
| + $^{191}Ir(n,\gamma)$ | 77193.703 | Calculated | | 375.0 ± 1% | 157.9 ± 1% | 53.54 ± 1% | 16.95 ± 1% | 3.068 ± 1% |
| | 77191.713 | | | | | | | |
| $^{193}Ir(n,n')$ | | Experiment | | 61 ± 15% | 33 ± 25% | 15 ± 50% | 8 ± 100% | |
| | 77193.703 | Calculated | | 78.39 ± 1% | 40.73 ± 1% | 16.25 ± 1% | 5.604 ± 1% | |
| $^{235}U(n,f)$ | | Experiment | | 829 ± 3% | 374 ± 3% | 142 ± 3% | 46.0 ± 3% | 8.67 ± 4% |
| | 92238.713 | Calculated | | 779.4 ± 1% | 375.2 ± 3% | 141.0 ± 2% | 47.17 ± 2% | 9.051 ± 5% |
| | 92235.50 | Calculated | | 773.4 ± 1% | 370.8 ± 2% | 138.5 ± 3% | 46.14 ± 2% | 8.862 ± 4% |
| $^{238}U(n,f)$ | | Experiment | 2285 ± 3% | 369 ± 3% | 150 ± 3% | 46.7 ± 3% | 13.0 ± 4% | 3.26 ± 5% |
| | 92238.713 | Calculated | 1920 ± 0% | 362.1 ± 1% | 151.2 ± 3% | 45.28 ± 3% | 12.82 ± 2% | 3.307 ± 6% |
| | 92238.50 | Calculated | 1824 ± 0% | 345.4 ± 1% | 144.6 ± 3% | 43.46 ± 3% | 12.35 ± 2% | 3.194 ± 6% |

(Continued)

TABLE V (Continued)

RADIOCHEMICAL ACTIVATION
EXPERIMENTALLY OBSERVED[a] AND CALCULATED[b] VALUES ($\times 10^{13}$)
(ENDF/B-V TRANSPORT CROSS SECTIONS)

| Reaction | Activation[c,d] Cross Section | Notes | Distance from Source (cm) 2.22 | 5.00 | 7.615 | 12.60 | 20.00 | 30.00 |
|---|---|---|---|---|---|---|---|---|
| $^{45}Sc(n,\gamma)$ | | Experiment | | 3.508 ± 3% | 2.492 ± 3% | 1.363 ± 3% | 0.5511 ± 3% | 0.0971 ± 7% |
| | 21045.713 | Calculated | | 3.171 ± 3% | 2.425 ± 3% | 1.334 ± 3% | 0.5392 ± 2% | 0.0697 ± 2% |
| $^{89}Y(n,\gamma)$ | | Experiment | 4.592 ± 3% | 2.029 ± 3% | 1.301 ± 3% | 0.6687 ± 3% | 0.2562 ± 3% | 0.0348 ± 3% |
| | 39089.113[h] | Calculated | 4.995 ± 1% | 1.894 ± 2% | 1.248 ± 2% | 0.6550 ± 2% | 0.2613 ± 2% | 0.0354 ± 2% |
| $^{169}Tm(n,\gamma)$ | | Experiment | | 59.80 ± 3% | 44.75 ± 3% | 24.38 ± 3% | 10.04 ± 3% | 1.974 ± 10% |
| | 69169.713 | Calculated | | 60.02 ± 2% | 47.18 ± 1% | 29.53 ± 1% | 12.48 ± 1% | 1.483 ± 1% |
| $^{197}Au(n,\gamma)$ | | Experiment | 72.35 ± 3% | 50.63 ± 3% | 36.44 ± 3% | 19.81 ± 3% | 8.126 ± 3% | 1.068 ± 3% |
| | 79197.713 | Calculated | 67.81 ± 4% | 45.42 ± 2% | 35.77 ± 2% | 21.54 ± 2% | 8.948 ± 2% | 1.040 ± 2% |
| | 79197.50 | Calculated | 47.55 ± 6% | 38.16 ± 3% | 31.25 ± 3% | 18.93 ± 2% | 7.897 ± 2% | 0.8993 ± 2% |
| $^{238}U(n,\gamma)$ | | Experiment | 46.11 ± 3% | 29.75 ± 3% | 20.87 ± 3% | 11.14 ± 3% | 4.476 ± 3% | 0.5841 ± 3% |
| | 92238.713 | Calculated | 30.86 ± 7% | 22.62 ± 3% | 17.41 ± 2% | 10.61 ± 3% | 4.151 ± 2% | 0.5173 ± 2% |
| | 92238.50 | Calculated | 31.22 ± 6% | 23.53 ± 2% | 18.39 ± 2% | 11.08 ± 3% | 4.470 ± 3% | 0.5535 ± 2% |
| | 92238.553[i] | Calculated | 42.83 ± 4% | 27.20 ± 2% | 20.47 ± 3% | 11.98 ± 3% | 4.788 ± 3% | 0.6125 ± 3% |

[a]Experimental values taken from Ref. 5.

[b]Calculated using a three-dimensional model (described in the section on Radiochemical Detection Foils) and ENDF/B-V cross sections for transport as described in footnote on page 8.

[c]The number to the left of the decimal is the MCNP nuclide identification number (atomic number followed by mass number). The number to the right of the decimal is the neutron cross-section set identifier.

[d]Activation cross sections identified by .703 and .713 are cross-section sets used in LA-7310. They are described in P. Soran, Los Alamos Internal Document, Table I (June 16, 1981). The .703 and .713 were used in the present work for cases where ENDF/B-V cross sections were not available or in addition to those of ENDF/B-V. Cross-section sets identified by .50 are those of ENDF/B-V.

[e]Experimentally observed foil activation (activations produced per foil atom by $9.42 \times 10^{15}$ source neutrons).

[f]Uncertainties in precision on experimental values are those quoted in [a] above.

[g]Statistical uncertainties in the calculated values are for one standard deviation.

[h]Cross-section file 39089.113 is a specially prepared activation file for MCNP $^{89}Y(n,\gamma)$ similar to that used in LA-7310. See footnote on page 9.

[i]Cross-section file 92238.553 is a specially prepared modified ENDF/B-V $^{238}U(n,\gamma)$ activation file. It consists of ENDF/B-V up to 30 keV; the values found in the paper: W. P. Poenitz, L. R. Fawcett, Jr., and D. L. Smith, Nuclear Science and Engineering 79, 239-247 (1981) from 30 keV up to 1.106 MeV; and beyond 1.106 MeV, an arbitrary straight line (on a log-log scale) with slope such that the modified cross section is 6.8 mb at 14 MeV.

TABLE VI

RATIO OF OBSERVED-TO-CALCULATED[a] RADIOCHEMICAL ACTIVATION
(ENDF/B-V TRANSPORT CROSS SECTIONS)

| Reaction | Activation[b,c] Cross Section | Distance from Source (cm) 2.22 | 5.00 | 7.615 | 12.60 | 20.00 | 30.00 |
|---|---|---|---|---|---|---|---|
| $^{89}Y(n,2n)$ | 39089.713 | 1.255 ± 3%[d] | 1.003 ± 4% | 1.007 ± 4% | 0.953 ± 6% | 0.995 ± 4% | 0.899 ± 4% |
| $^{90}Zr(n,2n)$ | 40090.703 | | 0.962 ± 4% | 0.961 ± 4% | 0.926 ± 5% | 0.845 ± 4% | 0.769 ± 9% |
| $^{169}Tm(n,2n)$ | 69169.713 | | 0.981 ± 4% | 0.974 ± 4% | 0.983 ± 6% | 0.971 ± 4% | 0.915 ± 4% |
| $^{191}Ir(n,2n)$ | 77191.713 | | 0.999 ± 3% | 0.893 ± 4% | 0.927 ± 4% | 0.839 ± 8% | 0.818 ± 8% |
| $^{197}Au(n,2n)$ | 79197.713 | 1.134 ± 3% | 0.978 ± 3% | 0.883 ± 4% | 0.944 ± 4% | 0.845 ± 8% | 0.859 ± 4% |
| | 79197.50 | 1.140 ± 3% | 0.986 ± 3% | 0.892 ± 4% | 0.958 ± 4% | 0.861 ± 8% | 0.879 ± 4% |
| $^{238}U(n,2n)$ | 92238.713 | 1.145 ± 3% | 1.114 ± 4% | 1.031 ± 6% | 1.058 ± 6% | 1.101 ± 4% | 0.925 ± 10% |
| | 92238.50 | 1.168 ± 3% | 1.148 ± 4% | 1.075 ± 6% | 1.111 ± 5% | 1.160 ± 4% | 0.980 ± 10% |
| $^{193}Ir(n,2n)$ + $^{191}Ir(n,\gamma)$ | 77193.703 + 77191.713 | | 1.070 ± 3% | 1.056 ± 3% | 0.972 ± 3% | 0.953 ± 3% | 0.968 ± 7% |
| $^{193}Ir(n,n')$ | 77193.703 | | 0.78 ± 15% | 0.81 ± 25% | 0.92 ± 50% | 1.43 ± 100% | |
| $^{235}U(n,f)$ | 92235.713 | | 1.064 ± 3% | 0.997 ± 4% | 1.007 ± 4% | 0.975 ± 4% | 0.958 ± 6% |
| | 92235.50 | | 1.072 ± 3% | 1.009 ± 4% | 1.025 ± 4% | 0.997 ± 4% | 0.978 ± 6% |
| $^{238}U(n,f)$ | 92238.713 | 1.190 ± 3% | 1.019 ± 3% | 0.993 ± 4% | 1.031 ± 4% | 1.014 ± 5% | 0.986 ± 8% |
| | 92238.50 | 1.253 ± 3% | 1.068 ± 3% | 1.037 ± 4% | 1.075 ± 4% | 1.053 ± 5% | 1.021 ± 8% |

(Continued)

TABLE VI (Continued)

RATIO OF OBSERVED-TO-CALCULATED[a] RADIOCHEMICAL ACTIVATION
(ENDF/B-V TRANSPORT CROSS SECTIONS)

| Reaction | Activation[b,c] Cross Section | Distance from Source (cm) 2.22 | 5.00 | 7.615 | 12.60 | 20.00 | 30.00 |
|---|---|---|---|---|---|---|---|
| $^{45}Sc(n,\gamma)$ | 21045.713 | | 1.106 ± 4% | 1.028 ± 4% | 1.022 ± 4% | 1.022 ± 4% | 1.393 ± 7% |
| $^{89}Y(n,\gamma)$ | 39089.113[e] | 0.919 ± 4% | 1.071 ± 4% | 1.050 ± 4% | 1.021 ± 4% | 0.980 ± 4% | 0.984 ± 4% |
| $^{169}Tm(n,\gamma)$ | 69169.713 | | 0.996 ± 4% | 0.948 ± 3% | 0.826 ± 3% | 0.804 ± 3% | 1.331 ± 10% |
| $^{197}Au(n,\gamma)$ | 79197.713 | 1.055 ± 5% | 1.115 ± 4% | 1.019 ± 4% | 0.920 ± 4% | 0.908 ± 4% | 1.027 ± 4% |
| | 79197.50 | 1.505 ± 7% | 1.327 ± 4% | 1.166 ± 4% | 1.046 ± 4% | 1.029 ± 4% | 1.188 ± 4% |
| $^{238}U(n,\gamma)$ | 92238.713 | 1.466 ± 8% | 1.315 ± 4% | 1.199 ± 4% | 1.050 ± 4% | 1.078 ± 4% | 1.129 ± 4% |
| | 92238.50 | 1.449 ± 7% | 1.265 ± 4% | 1.135 ± 4% | 1.005 ± 4% | 1.001 ± 4% | 1.055 ± 4% |
| | 92238.553[f] | 1.056 ± 5% | 1.094 ± 4% | 1.020 ± 4% | 0.930 ± 4% | 0.933 ± 4% | 0.954 ± 4% |

[a]The neutron transport cross sections used to obtain calculated values are those of ENDF/B-V as described in footnote on page 8.

[b]The number to the left of the decimal is the MCNP nuclide identification number (atomic number followed by mass number). The number to the right of the decimal is the neutron cross section set identifier.

[c]Activation cross sections identified by .703 and .713 are cross-section sets used in LA-7310. They are described in P. Soran, Los Alamos Internal Document, Table I (June 16, 1981). The .703 and .713 cross sections were used in the present work for cases where either ENDF/B-V cross sections were not available or in addition to those of ENDF/B-V. Cross section sets identified by .50 are those of ENDF/B-V.

[d]The quoted errors were determined from a square root of the sum of the squares combination of the observed and calculated fractional uncertainties. (No estimates of cross-section uncertainties are included.)

[e]Cross-section file 39089.113 is a specially prepared activation file for MCNP $^{89}Y(n,\gamma)$ similar to that used in LA-7310. See footnote on page 9.

[f]Cross section file 92238.553 is a specially prepared modified ENDF/B-V $^{238}U(n,\gamma)$ activation file. It is composed as follows:

| | | | |
|---|---|---|---|
| .001 | - | 30 keV | ENDF/B-V |
| 30 | - | 1.106 keV | W. P. Poenitz, L. R. Fawcett, Jr., and D. L. Smith, Nuclear Science and Engineering 78, 239-247 (1981). |
| 1.106 | - | 20 MeV | Straight line on a log-log scale through 119 mb at 1.106 MeV and 6.8 mb at 14 MeV. |

decreases in neutron energies correspond to very large decreases in cross-section values for these high-threshold-energy (n,2n) reactions.

The shapes of the (n,2n) plots strongly suggest an off-center neutron source. Moving the source off center and 2 mm closer to the foils solves the problem for (n,2n) at the 2.2-cm position; however, that move is detrimental to the previously fairly satisfactory ratios for $^{89}Y$ and $^{197}Au$ at larger radial distances. (See Table II.) Thus a slightly off-center source can be only partially responsible for the (n,2n) problem.

Finally, enough high-energy secondary neutrons from charged particle reactions may be produced to make a significant contribution to the observed activation values at shallow foil positions.

### 2. (n,f) Activation

Two sets of activation cross sections (ENDF/B-V and LA-7310) were used for this reaction. Both produced good results in all positions except for $^{238}U$ at 2.2 cm. Here again the calculated values were significantly less than the observed. As can be seen in Table II calculated activations with the source modeled 2 mm closer to the foils brought the 2.2-cm O/C value very close to unity without detriment to the ratios for deeper foils.

### 3. (n,γ) Activation

Here only the $^{89}Y(n,\gamma)$, $^{197}Au(n,\gamma)$ 79197.713 (see footnotes c, d, and i of Table V for identification), and $^{238}U(n,\gamma)$ 92238.553 results are acceptable; all others display undercalculation in either the shallow or deep penetration regions or both. $^{169}Tm(n,\gamma)$ shows overcalculation in the mid-penetration region. Modeling the neutron source 2 mm closer to the foils did not significantly reduce the undercalculation in the shallow penetration position. This is not surprising in light of (n,γ) cross sections being relatively small in the high-energy region. Thus increasing the exposure to 14-MeV neutrons adds little to calculated values.

The $^{197}Au(n,\gamma)$ 79197.713 activation cross-section file, which produces acceptable results, has the same shape as that of ENDF/B-IV, but is everywhere 6% larger. The newer evaluation, ENDF/B-V, identified in Tables V and VI by 79197.50, is much lower in the high-energy region. At 14 MeV the

ENDF/B-V evaluation is smaller than that of ENDF/B-IV by a factor of 10. At 9 MeV it is smaller by a factor of 39. Using the ENDF/B-V (n,γ) file results in grossly undercalculated values in the shallow penetration region.

For $^{238}$U(n,γ) both the cross section sets 92238.713 and 92238.50 produce large undercalculation at small radial positions. However, the modified cross-section set 92238.553 (described in note f of Table VI) produces acceptable results at all foil positions. The results from 92238.553 demonstrate the sensitivity of calculated activation to changes in the $^{238}$U(n,γ) cross section at the high-energy end. This cross-section file is composed of what the writer believes to be the most reliable data up to 1.1 MeV. Beyond 1.1 MeV the cross-section values were arbitrarily chosen based on an educated guess as to what the high-energy cross-section values must be to produce acceptable calculated activation. The modified and ENDF/B-V $^{238}$U(n,γ) cross sections are compared in Fig. 6.

Figures 5a through 5n are graphs of data taken from Table VI.

## V. CONCLUSIONS

Although results from the radiochemical activation part of this reanalysis leave much to be desired, the tritium production results for both $^{6}$Li and $^{7}$Li are quite acceptable. The use of ENDF/B-V cross sections for both neutron transport and tritium production and the modeling of ampules with correct radii and filled with the same mass of LiH as in the experiment produce calculated values close to the experimental values. When one takes into consideration the uncertainties for each ampule associated with the experimental (6% systematic plus 6% statistical[2]) and calculated values (2%-9% statistical), the observed-to-calculated ratios are remarkably close to unity.

Why the foil results are not comparable in quality to those for tritium production remains unanswered. We are convinced that our MCNP input model faithfully reproduced the geometry and conditions of the experiment (except for the beam, α-monitor and target insertion channels, stems on the ampules, and the possibility of an off-center neutron source). This statement is substantiated by the fact that when we used the same cross sections employed in the original analysis we were able to reproduce those observed-to-calculated foil activation ratios to a high degree of precision.

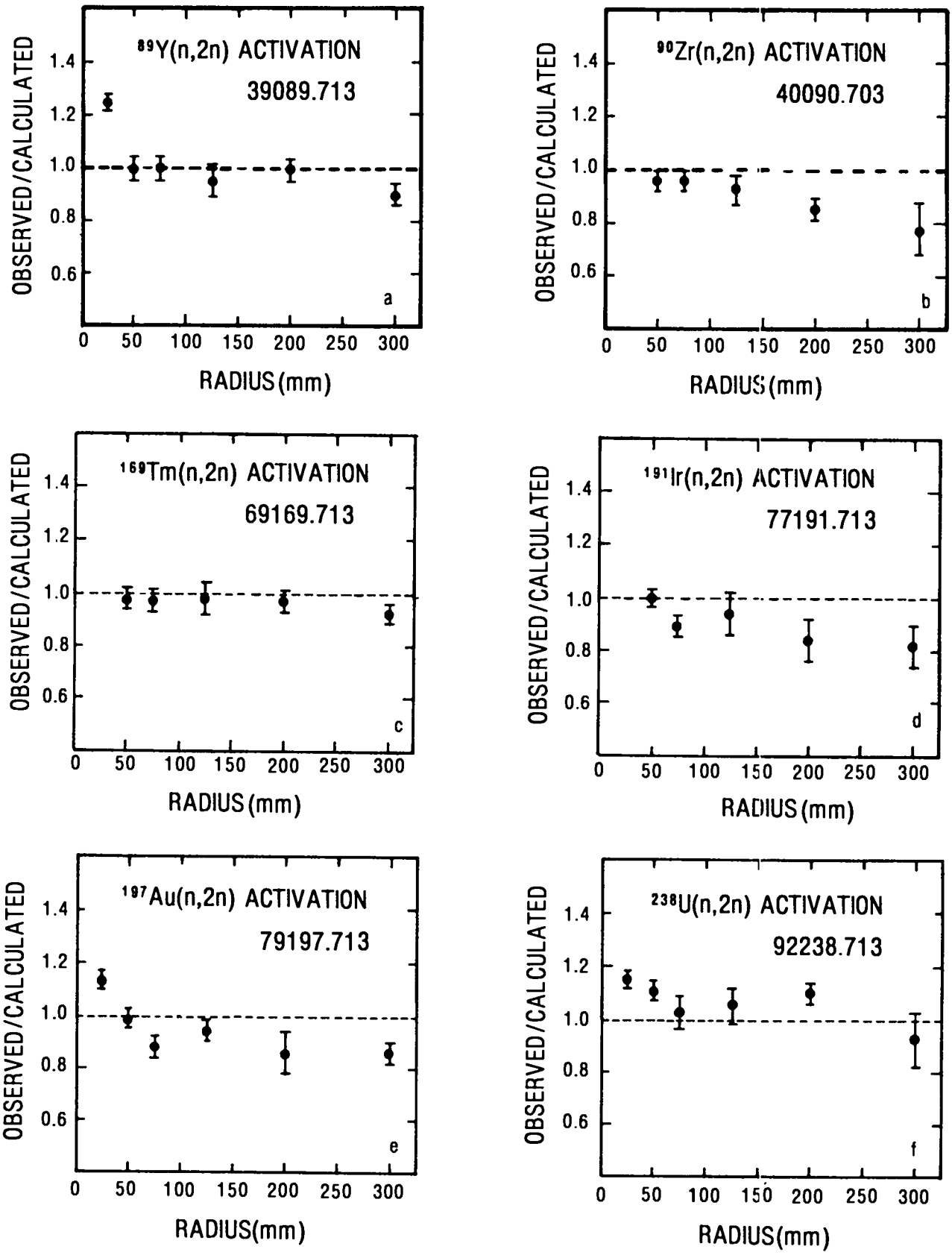


Fig. 5. Ratio of observed-to-calculated activation at the foil positions.

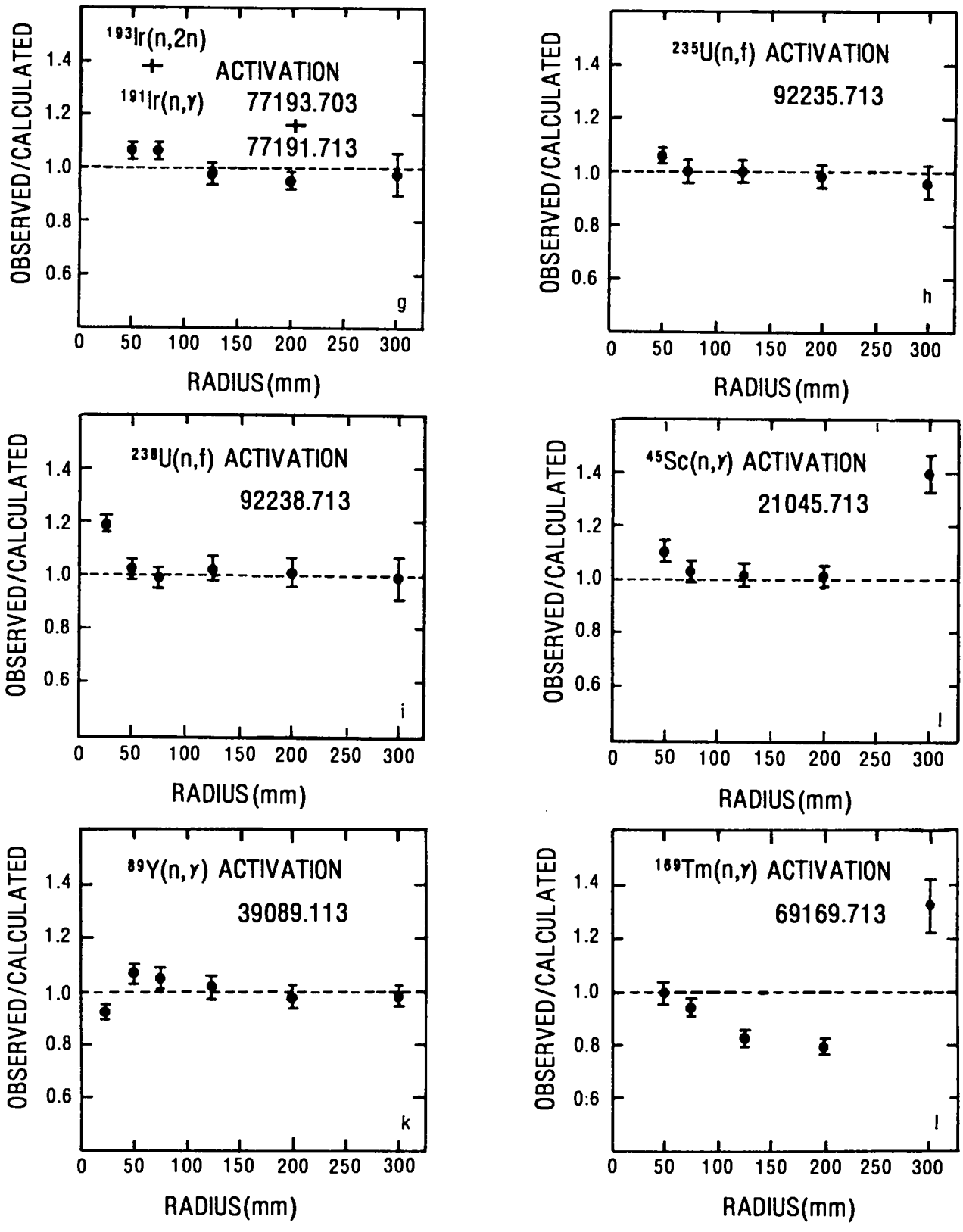


Fig. 5. (Cont.). Ratio of observed-to-calculated activation at the foil positions.

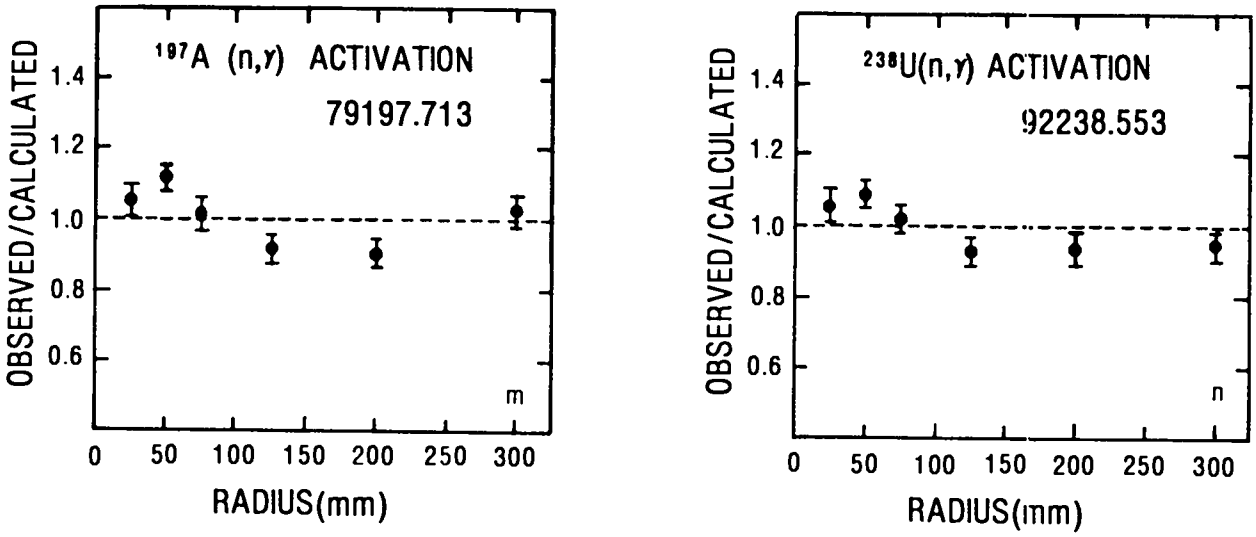


Fig. 5. (Cont.). Ratio of observed-to-calculated activation at the foil positions.

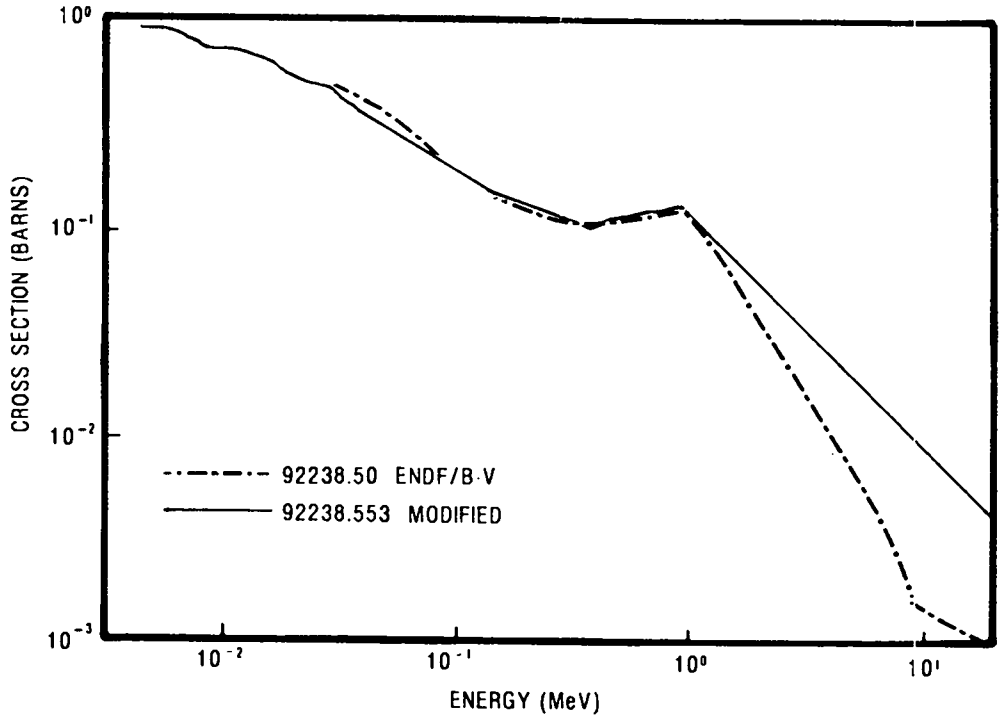


Fig. 6. Comparison of $^{238}U(n,\gamma)$ cross sections.

The investigation of several factors (self-activation, room return, and off-center source) that may have influenced the experimental results failed, with one exception, to materially improve the observed-to-calculated ratios. The one exception was the off-center calculation. Here the (n,2n) and (n,f) ratios at the 2.2-cm position were brought very close to unity. However. for

foils in the 5-, 7.6-, and 12.6-cm positions, the new (n,2n) calculated values were generally too large for $^{89}Y$ and $^{197}Au$. For those observed-to-calculated values of (n,γ) that were larger than one in the 2.2-cm position, moving the source off center reduced these ratios by only 3 to 4%, and the ratios for the more distant foils were essentially unchanged. In light of these several observations it can be concluded that although an off-center neutron source may have contributed to O/C ratios for (n,2n) reactions in the 2.22-cm position being larger than one, unidentified problems remain with some of the other O/C values that are still far from unity.

Use of the most recent ENDF/B-V cross-section sets for neutron transport in $^{6}LiD$ and for foil activation (in cases where they were available) failed to improve observed-to-calculated ratios and in some cases made them worse. If subsequent (n,2n) and (n,γ) cross-section evaluations for $^{197}Au$ and $^{238}U$ are larger in the 14-MeV region, one would expect some general improvement in their observed-to-calculated ratios.

Finally, the effect of secondary neutrons born from charged particle reactions needs to be investigated. As mentioned earlier, it is known that charged particle generation in this $^{7}LiD$ assembly is prolific. Unknown is whether the number of neutrons born from these charged particles is significant. Since MCNP currently does not transport charged particles, this question must remain unanswered for now.

## ACKNOWLEDGMENTS

The author is grateful to Robert Schrandt, Robert Seamon, Robert Little, and Guy Estes for their assistance. He is particularly grateful to Raymond Hunter, who arranged for the author's participation.

## REFERENCES

1. Marvin E. Wyman, "An Integral Experiment to Measure the Tritium Production from $^{7}Li$ by 14-MeV Neutrons in a Lithium Deuteride Sphere," Los Alamos Scientific Laboratory report LA-2234 (Rev.) (November 1972).

2. A. Hemmendinger, C. E. Ragan, E. R. Shunk, A. N. Ellis, J. M. Anaya, and Jon M. Wallace, "Tritium Production in a Sphere of $^{6}$LiD Irradiated by 14-MeV Neutrons," Los Alamos Scientific Laboratory report LA-7310 (October 1978). An abbreviated form was published in N.S.E. 70, 274-280, (1979).

3. Los Alamos Monte Carlo Group, "MCNP-A General Monte Carlo Code for Neutron and Photon Transport," Los Alamos National Laboratory report LA-7396-M (Rev.) (April 1981).

4. Eugene Goldberg, "HOTSPUR MEMO: Analysis of LANL Tritium Production Experiment (Bluebeard 1) with TART," Tables I & II, (January 27, 1982). Available from Eugene Goldberg, Lawrence Livermore National Laboratory.

5. D. W. Barr, "Report of CNC-11 Results on Bluebeard Sphere Experiment," Los Alamos Scientific Laboratory memorandum, Table I (May 27, 1976). Available from D. W. Barr, Los Alamos National Laboratory.

6. P. R. Bevington, Data Reduction and Error Analysis for the Physical Sciences (McGraw-Hill, New York, 1969), p. 71.

# APPENDIX A

## Typical Tritium Production Input File

```
1MCNP     VERSION BB2B  07/14/81        9450CC10N2 T 07/14/83  16:00:35
 ***********************************************************************
 INP      =        TLI6D

    1-       TRITIUM PRODUCTION IN LI6
    2-       1    0           -1
    3-       4    4  -0.743    1    -4   106   110
    4-       6    4  -0.743    4    -6   106   110   111   104
    5-       8    4  -0.743    6    -8   111   104   143   141   142
    6-       10   4  -0.743    8   -10   141   142   143   138   139   140
    7-       12   4  -0.743   10   -12   138   139   140   136   137   145
    8-       21   0           12   136   137   145
    9-       136  5  -0.363        -136
   10-       137  5  -0.346        -137
   11-       145  5  -0.342        -145
   12-       138  5  -0.31        -138
   13-       139  5  -0.33        -139
   14-       140  5  -0.35        -140
   15-       141  5  -0.33        -141
   16-       142  5  -0.32        -142
   17-       143  5  -0.36        -143
   18-       104  5  -0.27        -104
   19-       111  5  -0.23        -111
   20-       106  5  -0.27        -106
   21-       110  5  -0.26       -110
   22-
   23-       1    SO   2.230
   24-       4    SO   5.001
   25-       6    SO   7.616
   26-       8    SO  12.602
   27-       10   SO  20.002
   28-       12   SO  30.002
   29-       136  S  -26.44  10.24  -9.624  0.9
   30-       137  S  -26.44 -10.24  -9.624  0.9
   31-       145  S   19.90  21.18   7.244  0.9
   32-       138  S  -18.29  -5.215 -6.657  0.9
   33-       139  S  -15.51 -11.56  -5.645  0.9
   34-       140  S   15.51 -11.56   5.645  0.9
   35-       141  S  -10.37  -6.375 -3.776  0.9
   36-       142  S    8.472 -9.016  3.084  0.9
   37-       143  S  -10.21   6.275 -3.718  0.9
   38-       104  S   -4.185 -6.360 -1.523  0.5
   39-       111  S   -5.518  4.928 -2.009  0.5
   40-       106  S   -3.402 -3.620 -1.238  0.5
   41-       110  S   -2.990  3.792 -1.088  0.5
   42-
   43-       IN   1 1 1 1 1 2 0 4 12R
   44-       MODE 0
   45-       SRC  .2 1 .4889 14.13 0 0 0 0 .5201 14.13 .5105 14.13 0
   46-       FILES 14 BBSRC
   47-       E0   1-6 1-5 1-4 1-3 1-2 1-1 2-1 5-1 1.0 2.0 5.0 10.0 13.0 15.5 20.0
   48-       F4   136 137 145 138 139 140 141 142 143 104 111 106 110
   49-       FM4  0.942E-8  1  205
   50-       F24  136 137 145 138 139 140 141 142 143 104 111 106 110
   51-       FM24 0.942E-8  2  205
   52-       M1   3006.50  1.0
   53-       M2   3007.55  1.0
   54-       M4   1002.55  0.5    3006.50  0.4782    3007.55  0.0218
   55-       M5   1001.50  0.5   3006.50  0.4775   3007.55  0.0225
   56-       NPS  300000
   57-       CTME 60
   58-       TOTNU
   59-       ERGN 0  20.0
   60-       CUTN 1.0E123 1.0E-7 -0.1  -0.05
```

## APPENDIX B

Ratio of Observed-to-Calculated[a] Radiochemical Activations:
A Comparison of the Present Work (Based on LA-7310 Cross Sections)
and the Results from LA-7310

| Reaction | Activation Cross Section | Notes | Distance from Source (cm) 2.22 | 5.00 | 7.615 | 12.60 | 20.00 | 30.00 |
|---|---|---|---|---|---|---|---|---|
| $^{89}Y(n,2n)$ | 39089.713[b] | LA-7310[c] | 1.256 | 1.035 | 1.039 | 0.984 | 1.020 | 0.966 |
| | " | Present Work | 1.254 | 1.037 | 0.979 | 1.002 | 0.985 | 0.907 |
| $^{90}Zr(n,2n)$ | 40090.703[2] | LA-7310 | | 0.983 | 0.992 | 0.941 | 0.849 | 0.819 |
| | " | Present Work | | 0.995 | 0.948 | 0.962 | 0.829 | 0.773 |
| $^{169}Tm(n,2n)$ | 69169.713 | LA-7310 | | 1.004 | 0.997 | 1.003 | 0.992 | 0.973 |
| | " | Present Work | | 0.993 | 0.934 | 1.019 | 0.956 | 0.940 |
| $^{191}Ir(n,2n)$ | 77191.713 | LA-7310 | | 0.999 | 0.984 | 0.921 | 0.916 | 0.875 |
| | " | Present Work | | 0.989 | 0.922 | 0.936 | 0.883 | 0.846 |
| $^{197}Au(n,2n)$ | 79197.713 | LA-7310 | 1.135 | 0.979 | 0.974 | 0.939 | 0.925 | 0.919 |
| | " | Present Work | 1.128 | 0.970 | 0.912 | 0.954 | 0.892 | 0.887 |
| $^{238}U(n,2n)$ | 92238.713 | LA-7310 | 1.136 | 1.102 | 1.057 | 1.032 | 1.058 | 1.085 |
| | " | Present Work | 1.118 | 1.080 | 1.025 | 1.011 | 1.064 | 1.012 |
| $^{193}Ir(n,2n)$ | 77193.703 | LA-7310 | | 1.061 | 1.062 | 0.994 | 1.007 | 1.046 |
| $^{191}Ir(n,\gamma)$ | 77191.713 | Present Work | | 1.067 | 1.060 | 0.993 | 0.998 | 1.028 |
| $^{193}Ir(n,n')$ | 77193.713 | LA-7310 | | 0.744 | 0.793 | 0.908 | 1.453 | |
| | " | Present Work | | 0.748 | 0.750 | 0.888 | 1.390 | |
| $^{235}U(n,f)$ | 92235.713 | LA-7310 | | 1.030 | 1.001 | 1.004 | 0.989 | 1.047 |
| | " | Present Work | | 1.016 | 0.961 | 0.987 | 0.943 | 0.981 |
| $^{238}U(n,f)$ | 92238.713 | LA-7310 | 1.163 | 0.992 | 0.999 | 0.998 | 0.995 | 1.121 |
| | " | Present Work | 1.172 | 0.969 | 0.968 | 0.932 | 0.970 | 0.997 |
| $^{45}Sc(n,\gamma)$ | 21045.713 | LA-7310 | | 1.054 | 1.077 | 1.084 | 1.085 | 1.438 |
| | " | Present Work | | 1.061 | 1.061 | 1.087 | 1.046 | 1.384 |
| $^{89}Y(n,\gamma)$ | 39089.113[d] | LA-7310 | 0.971 | 1.015 | 1.028 | 1.011 | 0.978 | 0.991 |
| | " | Present Work | 0.906 | 1.031 | 1.051 | 1.032 | 0.988 | 0.990 |
| $^{169}Tm(n,\gamma)$ | 69169.713 | LA-7310 | | 0.962 | 0.943 | 0.878 | 0.860 | 1.404 |
| | " | Present Work | | 0.973 | 0.930 | 0.865 | 0.827 | 1.346 |
| $^{197}Au(n,\gamma)$ | 79197.713 | LA-7310 | 1.026 | 1.059 | 1.041 | 0.983 | 0.964 | 1.079 |
| | " | Present Work | 1.034 | 1.099 | 1.032 | 0.973 | 0.939 | 1.031 |
| $^{238}U(n,\gamma)$ | 92238.713 | LA-7310 | 1.438 | 1.243 | 1.189 | 1.129 | 1.107 | 1.166 |
| | " | Present Work | 1.575 | 1.248 | 1.194 | 1.107 | 1.011 | 1.120 |

[a]The neutron transport cross sections used to obtain calculated values were the same as those employed in LA-7310. They were from the ENDF/B-III evaluation except for $^{2}H$ where the 1967 UK/Los Alamos evaluation was used.

[b]Activation cross sections identified by .703 and .713 are cross section sets used in LA-7310. They are described in: P. Soran, Los Alamos Internal Document, Table I (June 16, 1981).

[c]LA-7310, P.26, Table XII.

[d]Cross section set .113 is similar to that used in LA-7310 and is described by R. Little and R. Seaman, Los Alamos National Laboratory, "Cross Sections for $^{89}Y(n,\gamma)$," memorandum to L. R. Fawcett (July 21, 1981).

Printed in the United States of America
Available from
National Technical Information Service
US Department of Commerce
5285 Port Royal Road
Springfield, VA 22161

Microfiche (A01)

| Page Range | NTIS Price Code | Page Range | NTIS Price Code | Page Range | NTIS Price Code | Page Range |
|---|---|---|---|---|---|---|
| 001-025 | A02 | 151-175 | A08 | 301-325 | A14 | 451-475 |
| 026-050 | A03 | 176-200 | A09 | 326-350 | A15 | 476-500 |
| 051-075 | A04 | 201-225 | A10 | 351-375 | A16 | 501-525 |
| 076-100 | A05 | 226-250 | A11 | 376-400 | A17 | 526-550 |
| 101-125 | A06 | 251-275 | A12 | 401-425 | A18 | 551-575 |
| 126-150 | A07 | 276-300 | A13 | 426-450 | A19 | 576-600 |
| | | | | | | 601-up* |

*Contact NTIS for a price quote.

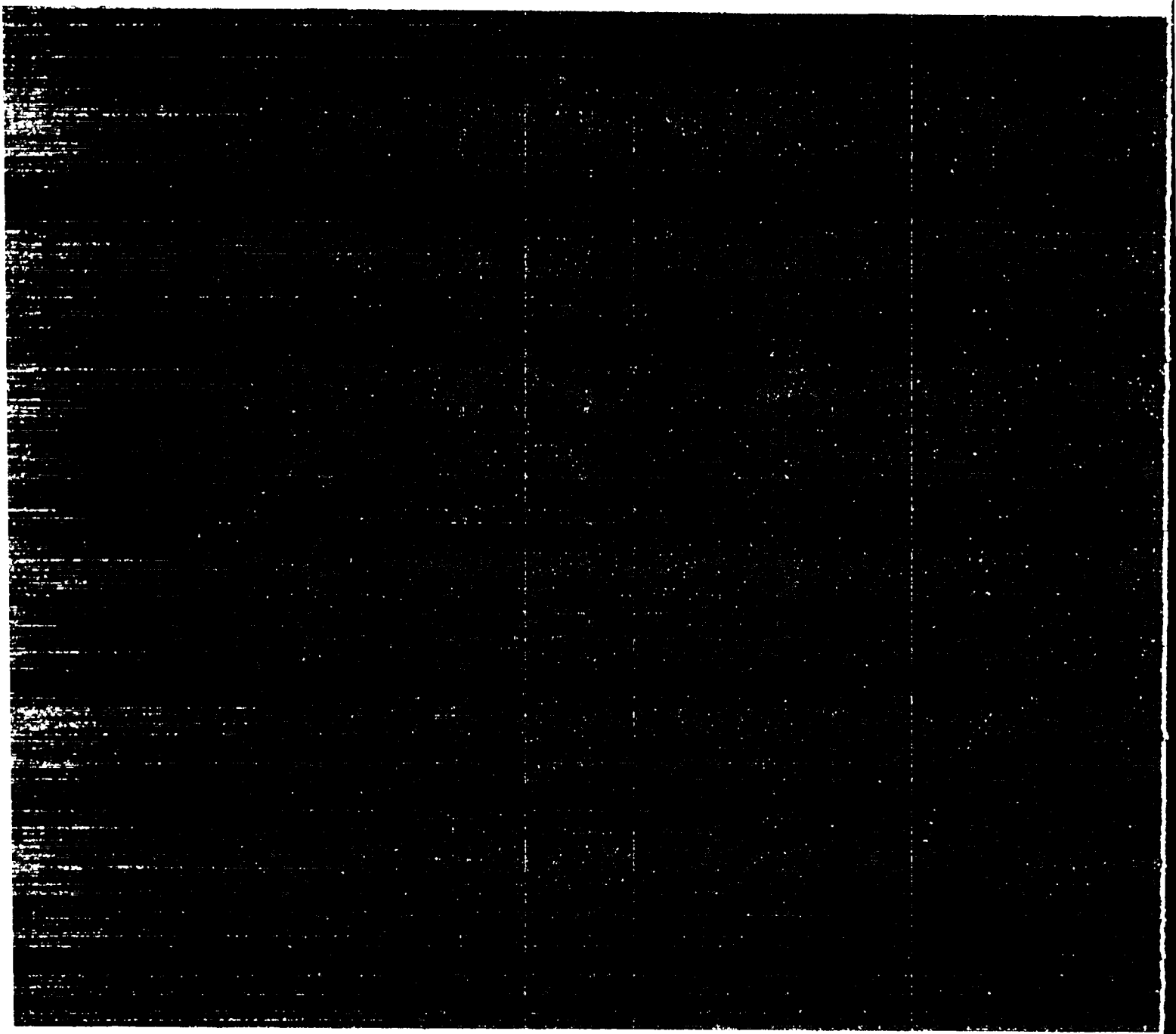

Los Alamos